Available online at www.sciencedirect.com

SciVerse ScienceDirect

Ceramics International 38 (2012) 6549–6556

CERAMICS INTERNATIONAL

www.elsevier.com/locate/ceramint

The effect of SiC addition on the crystallization kinetics of atmospheric plasma–sprayed basalt-based coatings

Ediz Ercenk[a,*], Ugur Sen[a], Senol Yilmaz[a,b]

[a]*Sakarya University, Engineering Faculty, Metallurgical and Materials Engineering Department, Esentepe Campus, 54187 Sakarya, Turkey*
[b]*TUBITAK-MAM, Material Institute, 41470 Gebze, Kocaeli, Turkey*

Received 19 July 2011; received in revised form 8 May 2012; accepted 14 May 2012
Available online 22 May 2012

Abstract

The crystallisation kinetics of the conversion of a glass coating layer made from a mixture of natural basalt volcanic rock and SiC into glass-ceramic have been investigated. The process depends on the crystallisation temperature, time and amount of the SiC added. Coating powders were prepared from pure basalt and from basalt containing 10–50 wt% SiC. The powders were coated by an atmospheric plasma spray technique on the pre-coated AISI 1040 steel substrate with Ni–Al. The coating layer was vitrified by sudden cooling. The amorphous structure of the coatings was verified by X-ray diffraction (XRD) analysis. To obtain glass-ceramic, coatings were subjected to crystallisation heat treatment in an argon atmosphere. Crystallisation heat treatment temperatures of 800 °C, 900 °C and 1000 °C were chosen by using DTA. After the heat treatment process, augite, ferrian-diopsite, diopside, albite, andesine, and moissonite phases formed in the coating layer and were verified by XRD analysis. The crystallisation activation energies were determined to be between 323.4 kJ/mol and 253.2 kJ/mol, depending on SiC addition. The crystallisation activation energies decreased with increasing amounts of SiC addition. The Avrami parameters of the crystallisation process varied between 1.60 and 3.33, which indicates that internal crystallisation dominated for all of the compositions.

Keywords: D: Glass-ceramic; D. SiC; Plasma spray coating; Crystallisation; Kinetics

1. Introduction

Basalt is a sort of natural volcanic structure that contains a high percentage of silicate. Chemically, it is composed of other oxides: Al_2O_3, Fe_2O_3, MgO, CaO and TiO_2. It is possible to prepare glass-ceramic from basalt because of the chemical composition. Basalt glass and glass-ceramics are suitable for commercial production, such as noise and thermal insulation systems. Basalt shows a high crystallisation tendency because of the iron oxides in the structure [1,2]. When the natural volcanic basalt rocks are ground into powder form, the powder can be used as a plasma spray coating powder. Glassy basalt coatings in the amorphous phase can be transformed into the glass-ceramic form with suitable heat treatment [2,3].

Glass-ceramics are fine-grained polycrystalline materials formed when glasses of suitable compositions are heat-treated and thus undergo controlled crystallisation to reach a lower-energy crystalline state [4]. This process includes crystallisation and crystalline growth steps. Crystallisation is affected by many parameters, such as heat treatment time, temperature, chemical composition and nucleation agents. The crystallisation kinetics of the high-temperature processes plays an important role in the determination of the process parameters, such as treatment temperature and times, for the desired conditions [5,6]. The activation energy of the glass crystallisation phenomena is associated with nucleation and growth processes. Kinetic studies are always connected with the concept of activation energy [3,7]. Differential thermal analysis (DTA) is a method to obtain crystallisation and viscous flow activation energies [2,3]. Thermally activated transformations in the solid state can be investigated by isothermal or non-isothermal experiments [7]. The main goal of the study

*Corresponding author. Tel.: +90 264 295 5768; fax: +90 264 295 5601.
E-mail address: ercenk@sakarya.edu.tr (E. Ercenk).

0272-8842/$36.00
http://dx.doi.org/10.1016/j.ceramint.2012.05.037

was to investigate the crystallisation kinetics of the basalt-based coatings, including SiC coatings realised by the atmospheric plasma spray (APS) coating technique.

2. Experimental procedure

Volcanic basalt rocks were obtained from the Konya region of Turkey, which has some volcanic formations. SiC powders (280 mesh size) were commercially supplied by Eczacibasi Co. (Turkey). The basalt rocks were turned into chunks and crushed with jaw and conic crushers. After the crushing and sieving process, basalt powders with particle sizes of 53 ± 45 μm were obtained. Chemical composition of basalt was analysed quantitatively using Perkin–Elmer 2300 atomic absorption spectroscopy, and the results are given in Table 1. Six different coating powders were prepared from the basalt and the SiC mixtures, which contained 10–50 wt% SiC. A SiC-free powder was also prepared. The substrate used in this study was AISI 1040 steel that was 20 mm in diameter and 5 mm in height. The surface of the substrates was grit-blasted with 35-grid alumina under a pressure of 2 bar, an angle of 45°, a spray distance of 50 mm and a flow rate of 2 kg min^{-1}, followed by ultrasonic cleaning in an ethyl alcohol and acetone solvent for 15 min and drying. The basalt and SiC mixtures were sprayed onto substrates with a bond coat by the APS coating technique using a manually controlled plasma spray system. Ni–5 wt% Al (METCO 450 NS) was selected as the bond coat powder to obtain thermal suitability between the substrate and the main coating layer. The plasma spray parameters are given in Table 2. The torch nozzle used for coatings was METCO 3 MB with a 6 mm alloyed Cu nozzle. The position of the injector relative to the nozzle exit was 90°. The injector is in the same axis as the torch. The powder unit of the injector was the METCO 3 MP powder feed unit. The coating operations were performed at room temperature. The coatings were found to be amorphous by the X-ray diffraction analysis (XRD) technique. Glass-ceramic-coated samples were prepared by applying suitable heat treatments that were planned according to DTA results of the amorphous coatings. Heat treatments were carried out at temperatures of 800, 900 and 1000 °C in an argon atmosphere by a Protherm tube furnace with a time ranging from 1 to 4 h to promote internal crystallisation. The crystallisation temperatures were selected from the DTA curve, depending on the endothermic and exothermic reaction temperatures. A JEOL 6060 scanning electron microscopy (SEM) system and X-ray diffraction (XRD) analysis using a Rigaku-type diffractometer with CuK_α radiation, which has a wavelength of 1.54056 Å to analyse phases present in the coatings over a 2θ range of 10–90°, were used to characterise the coated samples.

DTA and differential scanning calorimetry (DSC) are widely used in investigating the crystallisation kinetics of glasses and glass-ceramics. In this study, the crystallisation kinetics of basalt-based SiC-reinforced coatings were studied by DTA to determine the peak temperatures (glass transition and crystallisation) and to calculate activation energies for the crystallisation and the viscous flow. After crushing, pulverising and grinding the coatings on the steel substrate to a powder size of approximately 30 μm, the DTA experiments were performed by a TA instrument with heating rates of 5, 10 and 15 °C/min. All DTA experiments were carried out in an argon atmosphere up to 1000 °C temperature. Thus, the effect of SiC addition on the crystallisation kinetics of basalt-based glass-ceramics coatings was investigated.

3. Results and discussion

SEM analysis of the surface of the coating layers showed that the coating layer was compact and had a characteristic plasma spray coating structure. A SEM micrograph of the basalt-based 30 wt% SiC-reinforced glass-ceramic coating is given in Fig. 1. As can be seen in this figure, un-melted particles and porosity were observed in the coating. These structures are characteristic of thermal spray coatings [8]. The granular structures were determined by SEM analysis. It is possible that these granular particles occur because of sudden cooling of basalt glass after the plasma spray process. It is difficult to determine the SiC particles in the microstructure of SiC reinforced basalt base glass-ceramic coating, clearly. It is probable that the outer parts of the SiC particles were melted in the plasma flame and melted parts of the semi-melted particles were oxidised in the atmospheric conditions. This is because, XRD analysis

Table 2
Plasma spray coating parameters.

Coating parameter	Value
Plasma gun (MB)	3
Current (A)	500
Voltage (V)	64–70
Gas flow for Ar (l/min)	50
Gas flow for H (l/min)	15
Spray distance (mm)	130
Powder feed rate (g/min)	39
Carrier gas flow (l/min)	3–6

Table 1
Chemical composition of basalt.

Oxide	SiO_2	Al_2O_3	Fe_2O_3	CaO	MgO	K_2O	Na_2O	P_2O_5	LOI
(wt%)	45.88	18.2	9.95	9.28	6.62	1.64	4.76	1.04	2.63

of the composite structure cannot exhibit the SiC peak clearly, as a dominant phase on the patterns, but some trace peaks of the SiC can be shown on the basalt base coatings as coat. But SEM micrograph and energy dispersive spectroscopy (EDS) analysis shows the SiC particles on the fracture surface of the coating layer, clearly as shown in Fig. 2. The mechanism can be described as a sequence of different steps: basalt-SiC mixtures crystalline powders were performed on steel surface by APS process. Initially, crystalline powders transformed amorphous structure due to plasma effect of APS process. During the coating process, dissociation and oxidation of SiC happened because of the same effect. Dissociation of SiC and formation of a protective amorphous silica-based film occurred, SiC was surrounded with SiO_2 (glass form), and then controlled crystallisation heat treatment was performed to produce glass-ceramic structure. Thus, the glass-ceramic structure was formed and devitrification of the surface film with crystallisation in the form of Diopside, Augite and other phases realized. This result was presented in a previous study [9].

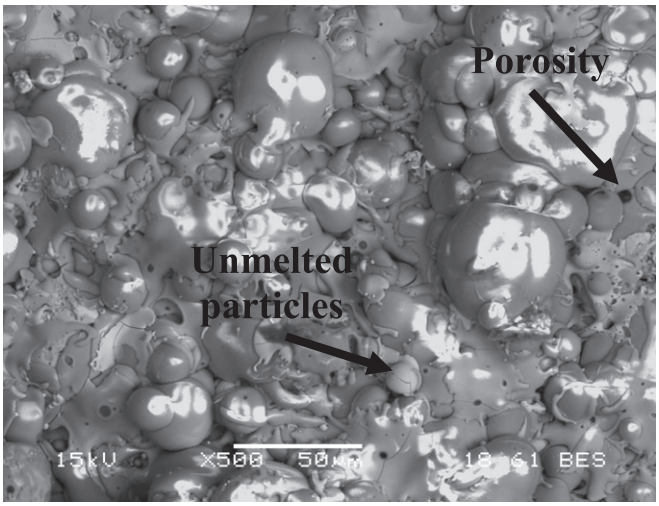

Fig. 1. Surface SEM micrograph of coating treated at 900 °C for 2 h.

After the APS process, XRD analysis results showed that the basalt-based SiC-reinforced and SiC-free coatings realised on the steel samples revealed an amorphous structure beside the some trace SiC phases (see Fig. 3). Basalt and SiC powders have a crystalline structure before the APS coating process, which is well explained in the earlier studies [9,10]. As shown in Fig. 3, all of the coatings have some very small peaks, but all of the XRD patterns have a background area that demonstrates the amorphous structures of the materials [11]. This structure is a characteristic of the glass structure before the glass-ceramic transformation treatment [12,13]. The basalt-based coatings, including SiC realised by APS coating, had a glassy structure, including some trace crystalline phases, which come from the un-melted or semi-melted powder particles. Glass-ceramic transformation was realized thanks to controlled heat treatment process. XRD analysis results of glass-ceramic coatings can be seen in Fig.4. Augite (ASTM

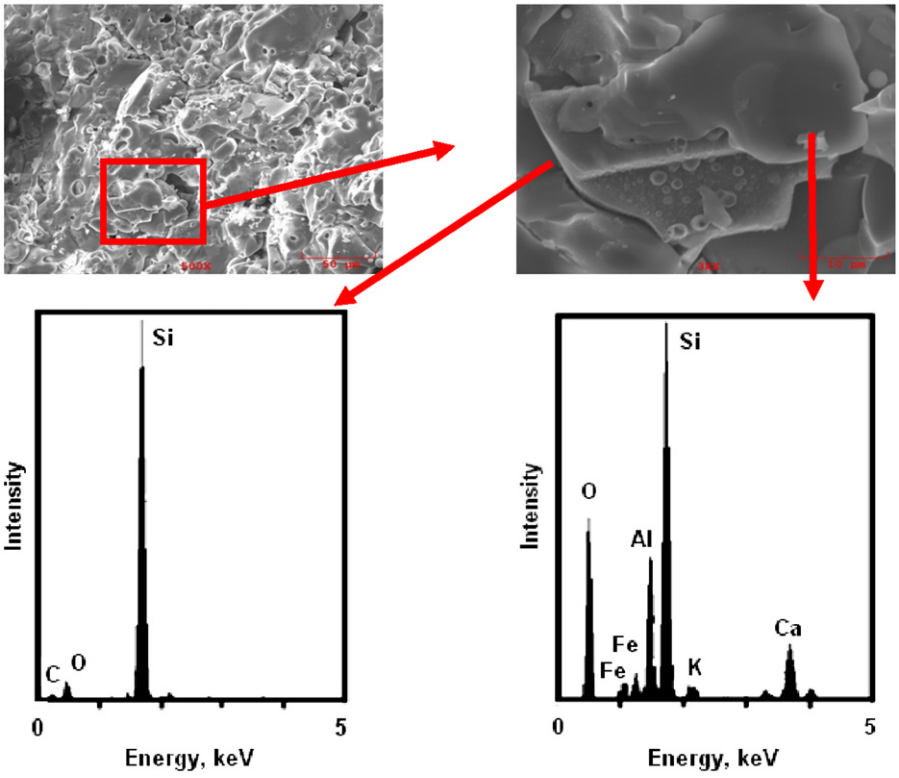

Fig. 2. SEM micrograph and EDS analyses of 10% SiC reinforced glass-ceramic coating with 800 °C for 2 h [9].

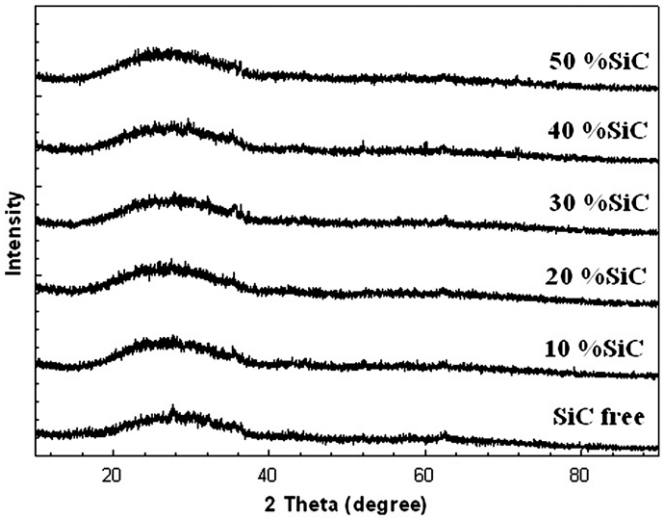

Fig. 3. XRD patterns of basalt based SiC reinforced glass coatings depending on SiC addition.

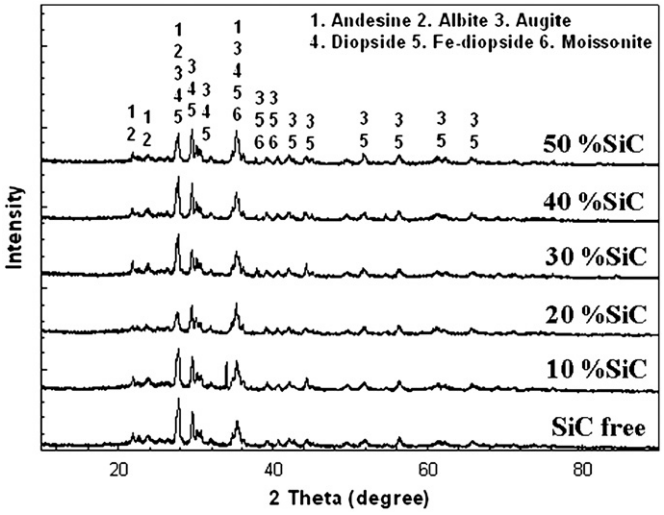

Fig. 4. XRD patterns of basalt based SiC reinforced glass-ceramic coatings depending on SiC addition.

chart no: 24-0203), Fe-diopside (ASTM chart no: 83-0100), diopside (ASTM chart no: 86-932), Albite (ASTM chart no: 41-1480), Andezine (ASTM chart no: 79-1148) and Moissonite (ASTM chart no: 72-1625) phases were determined after the crystallisation heat treatment in the XRD patterns of the basalt based glass-ceramic coatings.

For all of the powder compositions, DTA of the coating layer for as-coated conditions showed that the crystallisation temperature of the glass coatings realised at 800 °C revealed exothermic peaks (see Fig. 5). The crystallisation heat treatment temperatures of 800 °C, 900 °C and 1000 °C were determined from the DTA. These DTA curves have two or more exothermic peaks, which indicate that two or more phases appeared during the crystallisation treatment of the basalt-based coatings [2,3,14].

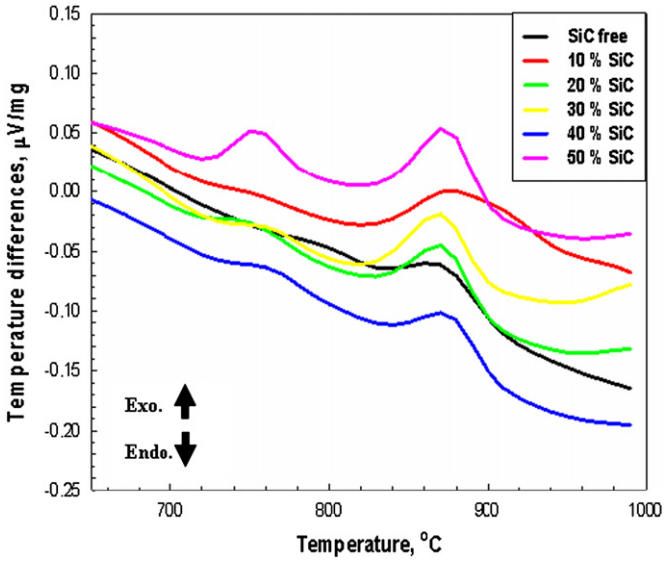

Fig. 5. DTA curves of SiC reinforced coating with heating rate 10 °C/min.

In the glass ceramics, the addition of nucleation agents increases the crystallisation amount of the glass ceramics. P_2O_5, TiO_2, Cr_2O_3, Fe_2O_3 and ZrO_2 are vital nucleation agents for this process [15,16]. In order to crystallise basalt-based glass-ceramics, nucleation agents are not necessary because the basalt itself contains some oxides, such as Fe_2O_3. In XRD patterns, the background zone represents the amorphous structure [11]. As can be seen from the XRD patterns, the addition of SiC resulted in higher crystalline peak intensities and lower background XRD patterns. The addition of SiC caused more heterogeneous nucleation surfaces. Hence, SiC affects the crystallisation as a heterogeneous nucleation agent [9].

DTA studies were performed on the glassy coatings to determine the crystallisation temperature by different heating rates. The variation of the crystallisation peaks with different DTA heating rates can be used to estimate the activation energy for crystallisation and to determine the crystallisation mechanism [17]. The endothermic peak indicates the glass transition, and the exothermic peaks correspond to the crystallisation reactions of the glass [18]. Fig. 4 shows DTA results of different heating rates with different SiC addition coatings. Glass transition temperatures (T_g) were determined between 987 K and 1047 K, depending on SiC addition. Crystallisation temperatures (T_p) were measured between 1134 K and 1147 K, depending on SiC addition. Different exothermic peaks on the same DTA curve indicate that more than one crystal phase forms [14]. This situation was confirmed by the XRD results. T_g and T_p temperatures were measured via DTA curves and are given in Table 3.

The kinetics for isothermal solid-state phase transformation can be described by the phenomenological Johnson–Mehl–Avrami (JMA) equation [19,20]

$$X = 1-[(-kt)^n] \quad (1)$$

Table 3
Characteristic DTA peak temperatures of glass samples.

Sample	Heating rate, β (C° min^{-1})	T_g (K) glass transition temp.	T_p (K) cryst. temp.	ΔT (K)
SiC	5	1004	1119	31
free	10	1047	1134	35
	15	1079	1154	33
10%	5	972	1119	41
SiC	10	993	1147	55
	15	1004	1151	44
20%	5	973	1119	45
SiC	10	987	1141	33
	15	1006	1155	40
30%	5	1000	1125	43
SiC	10	1006	1141	39
	15	1008	1165	42
40%	5	990	1120	43
SiC	10	994	1134	35
	15	1009	1160	36
50%	5	991	1121	31
SiC	10	998	1147	33
	15	1004	1165	45

Table 4
Values of parameter n for various crystallisation mechanisms [2,3,14].

Mechanism	n
Bulk nucleation	
Three-dimensional growth	4
Two-dimensional growth	3
One-dimensional growth	2
Surface nucleation	1

Eq. (2) is obtained by taking the logarithm of Eq. (1)

$$\ln[-\ln(1-X)] = n\ln k + \ln t \tag{2}$$

where X is the volume fraction of crystallisation after time t, n is the Avrami parameter (which depends on the growth direction number and the mechanism of nucleation and crystal growth given in Table 4) and k is the reaction rate constant (1/s) (which depends on both the nucleation rate and the growth rate) [21,22]. The equation defining k is given below

$$k = V\exp\left(\frac{-E_a}{RT}\right) \tag{3}$$

where V is a frequency factor (s^{-1}), E_a is the activation energy for crystallisation (J/mol), R is the gas constant (8.314 J/mol) and T is the absolute temperature (K) [21,22].

From the value of the activation energy (E_a), the Avrami parameter (n) can be calculated using the equation presented by the Augis and Bennett for non-isothermal analysis

$$n = \left(\frac{2,5}{\Delta T}\right)\left(\frac{T_p^2}{\frac{E_a}{R}}\right) \tag{4}$$

Table 5
n-Values of plasma spray coated basalt based SiC reinforced glass.

Sample	Heating rate (°C/min)	n	Mechanism
SiC free	5	2.60	Bulk nucleation
	10	2.36	Bulk nucleation
	15	2.59	Bulk nucleation
10% SiC	5	2.05	Bulk nucleation
	10	1.60	Bulk nucleation
	15	2.02	Bulk nucleation
20% SiC	5	1.97	Bulk nucleation
	10	2.79	Bulk nucleation
	15	2.37	Bulk nucleation
30% SiC	5	2.25	Bulk nucleation
	10	2.55	Bulk nucleation
	15	2.47	Bulk nucleation
40% SiC	5	2.31	Bulk nucleation
	10	2.91	Bulk nucleation
	15	2.96	Bulk nucleation
50% SiC	5	3.33	Bulk nucleation
	10	3.27	Bulk nucleation
	15	2.48	Bulk nucleation

where ΔT is the full width of the exothermic peak at the half-maximum intensity and T_p is the crystallisation peak temperature. Consequently, a sharp peak (small ΔT, large n) implies bulk crystallisation, while a broad peak (large ΔT, small n) signifies surface crystallisation [23,24]. The n-values, which were calculated using Eq. (4), are given in Table 5.

The reaction rate constant (k) in Eq. (3), therefore, is no longer a constant but is a function of time, and the transformation mechanism cannot be described by the simple JMA equation (Eq. (2)). A modified form of the JMA equation that takes into account the dependence of k on t is used for non-isothermal crystallisation. The value of the activation energy for crystallisation of amorphous glassy layer was determined using a modified form of the JMA equation. It was originally applied to crystallisation studies by Kissinger and modified by others [23–25]. This method is based on the dependence of the crystallisation peak temperature (T_p) on the DTA or DSC heating rate (β), as follows

$$\frac{\ln T_p^2}{\beta} = \frac{\ln E_a}{R} - \ln V_a + \frac{E_a}{RT_p} \tag{5}$$

Likewise, Eq. (5) can also be used to predict the viscous energy, as described by Mahadevan et al. [26]

$$\frac{\ln T_p^2}{\beta} = \frac{\ln E_c}{R} - \ln V_c + \frac{E_c}{RT_g} \tag{6}$$

here E_c is the corresponding activation energy for viscous flow, T_g is the glass transformation temperature, V_a is the frequency factor for crystallisation and V_c is the frequency factor for viscous flow. Plots of $\ln T_p^2/\beta$ versus $1/T_p$ and $\ln T_g^2/\beta$ versus $1/T_g$ obtained at various heating rates should be linear with slopes E_a/R and intercepts $[\ln(E_a/R) - \ln V_a]$ and $[\ln(E_c/R) - \ln V_c]$. Plots of $\ln T_p^2/\beta$ versus $1/T_p$ and $\ln T_g^2/\beta$ versus $1/T_g$ are given in Fig. 6. The

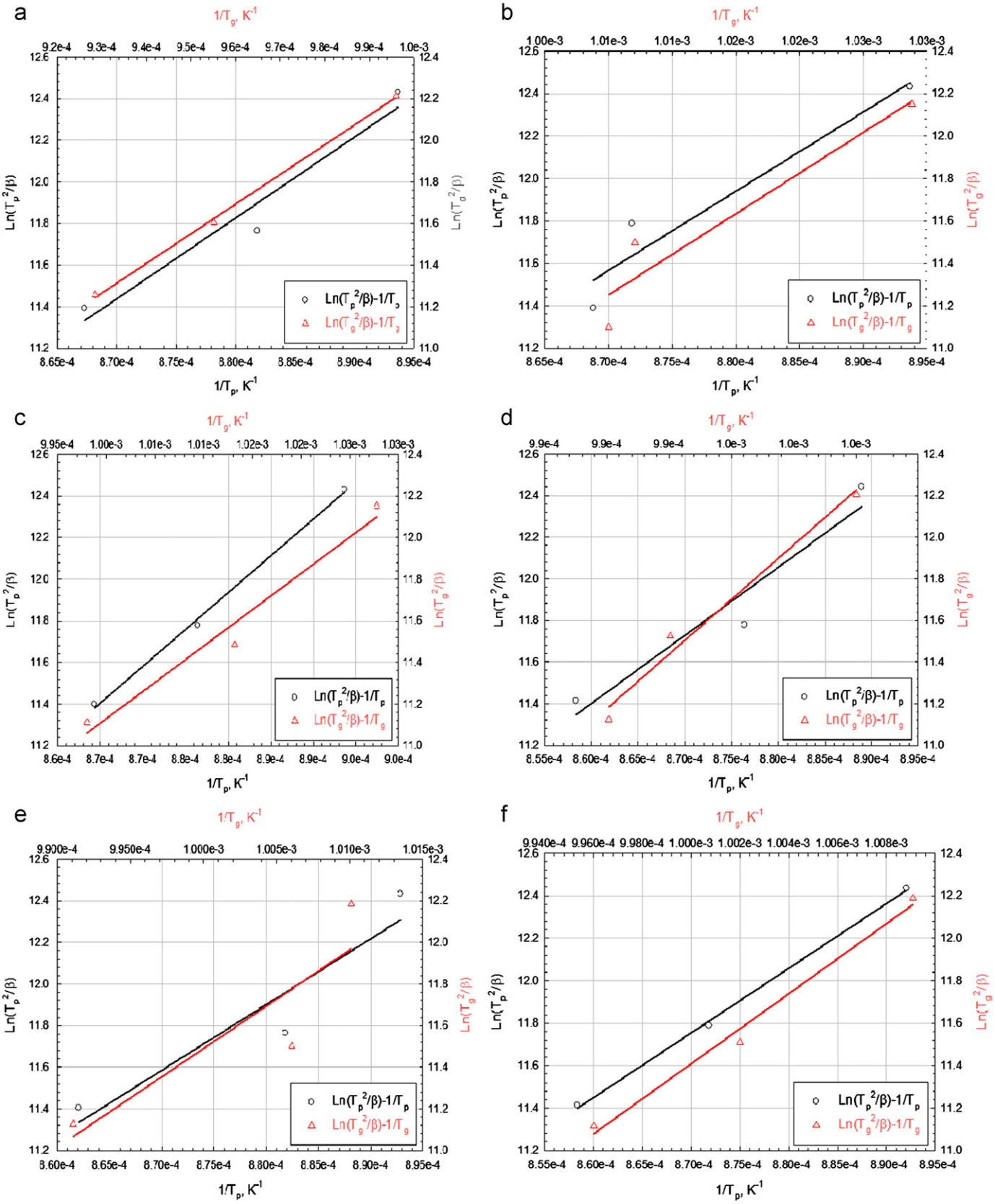

Fig. 6. Plots of ln T_p^2/β versus $1/T_p$ and ln T_g^2/β versus $1/T_g$ for the determination of the activation energy for the crystallisation and the viscous flow.

Table 6
The activation energy of the crystallisation and the viscous flow depending on SiC addition.

Samples	Crystallisation activation energy, E_a (kJ/mol)	Viscous flow activation energy, E_c (kJ/mol)
SiC free	323.4	118.5
10% SiC	310.3	318.6
20% SiC	293.8	290.1
30% SiC	272.2	1091.2
40% SiC	262.8	394.6
50% SiC	253.2	685.9

determined activation energy of the crystallisation and the viscous flow are given in Table 6.

The value of E_a is in good agreement with the study of Bayrak et al. [3]. However, it is not in good agreement with the values reported by Pacurariu et al. (E_a=231–283 kJ/mol) and Yilmaz et al. (E_a=238 kJ/mol) who studied the kinetics of crystallisation of pure basalt glass using the isothermal method [2,27]. This may be due to the complex crystallisation behaviours of the amorphous, glassy, basalt-based coatings formed from melted basalt glass [3].

The n-values, which were calculated using Eq. (4), are given in Table 5. It can be seen that n=1.60–3.33, which indicates that the crystallisation of the amorphous glassy basalt-based coatings at all heating rates is caused by bulk nucleation.

4. Conclusions

The effect of SiC addition on the crystallisation kinetic of basalt-based glass was investigated. The results of the present study can be summarised as follows:

1) The coating layer includes porosity and un-melted particles after atmospheric plasma spray coating. The visual and microstructure observations showed that SiC-reinforced basalt powders have an area of applicability as thermal spray powders.
2) SiC and basalt powders had a crystalline structure initially. The plasma caused to amorphous structure formation in the coating layer. A controlled heat treatment process of the coating layer was performed to transform to crystalline structure. These results highlighted the fact that coated samples, which have an amorphous structure, were transformed to crystalline structures by the heat treatment process. The presence of SiC in coating layer was observed as a trace phase in the XRD results, in addition to this, it was proved in SEM and EDS analysis of the coating layers. Augite, ferrian-diopsite, diopside, albite, andesine and moissonite phases were determined by XRD analysis.
3) SiC addition has a positive effect on the crystallisation process. It is possible that some of SiC addition subjected to dissociation and oxidation due to plasma effect of APS process. But, the detection of the SiC in the coating including 10% SiC by SEM and EDS results indicated that the SiC particles remain in existence despite of plasma effect in all coating compositions. SiC particles bring about heterogeneous nucleation in the glassy matrix. The crystallisation activation energies decreased as the amount of SiC increased.
4) Depending on the heating rate, the n-values were found to vary between 1.60 and 3.33, which indicates bulk nucleation in the amorphous, glassy, basalt-based coatings.
5) The activation energies of the crystallisation and viscous flow were calculated as 253.2–323.4 and 118.5–1091.2 kJ mol^{-1}, respectively.

Acknowledgements

The authors would like to express their gratitude to Sakarya University Engineering Faculty, and Prof. C. Bindal, the head of the Department of Metallurgy and Material Engineering for supporting this work. The authors express theirs grateful thanks to Technician Ersan Demir and Ebubekir Cebeci at Plasma Spray laboratory of Sakarya University in addition this study was supported by the SENKRON metal&ceramic coating Co. in Turkey.

References

[1] S. Ergul, F. Ferrante, P. Pisciella, A. Karamanov, M. Pelino, Characterization of basaltic tuffs and their applications for the production of ceramic and glass–ceramic materials, Ceramics International 35 (2009) 2789–2795.
[2] S. Yilmaz, O.T. Ozkan, V. Gunay, Crystallization kinetic of basalt glass, Ceramics International 22 (1996) 477–481.
[3] G. Bayrak, S. Yilmaz, Crystallization kinetics of plasma sprayed basalt coatings, Ceramics International 32 (2006) 441–446.
[4] H. Liu, H. Lu, D. Chen, H. Wang, H. Xu, R. Zhang, Preparation and properties of glass–ceramics derived from blast-furnace slag by a ceramic-sintering process, Ceramics International 35 (2009) 3181–3184.
[5] M.H. Lewis, Glasses and Glass-Ceramics, Chapman and Hall, London, 1989.
[6] A. Paul, Chemistry of Glasses, Chapman and Hall, London, 1990.
[7] M.A. El-Oyoun, Crystallization kinetics of the chalcogenide $Bi_{10}Se_{90}$ glass, Journal of Physics and Chemistry of Solids 61 (2000) 1653–1662.
[8] S. Brossard, P.R. Munroe, A.T.T. Tran, M.M. Hyland, Study of the splat formation for plasma sprayed NiCr on aluminum substrate as a function of substrate condition, Surface and Coatings Technology 204 (2010) 2647–2656.
[9] E. Ercenk, U. Sen, S. Yilmaz, Structural characterization of plasma sprayed basalt-SiC glass-ceramic coatings, Ceramics International 37 (2011) 883–889.
[10] S. Yilmaz, G. Bayrak, S. Sen, U. Sen, Structural characterization of basalt-based glass-ceramic coatings, Materials and Design 27 (2006) 1092–1096.
[11] X.Y. Liu, C.X. Ding, Plasma-sprayed wollastonite 2M/ZrO_2 composite coating, Surface and Coatings Technology 172 (2003) 270–278.
[12] C. Leroy, M.C. Ferro, R.C.C. Monteiro, M.H.V. Fernandes, Production of glass-ceramics from coal ashes, Journal of the European Ceramic Society 21 (2001) 195–202.

[13] Z.J. Wang, W. Ni, Y. Jia, L.P. Zhu, X.Y. Huang, Crystallization behavior of glass ceramics prepared from the mixture of nickel slag blast furnace slag and quartz sand, Journal of Non-Crystalline Solids 356 (2010) 1554–1558.
[14] V. Znidarsic, D. Kolar, The Crystallization of diabase glass, Journal of Materials Science 26 (1991) 2490–2494.
[15] G.H. Beall, H.L. Rittler, Basalt glass ceramics, American Ceramic Society Bulletin 55 (1976) 579–582.
[16] J.E. Shelby, Introduction to Glass Science and Technology, The Royal Society and Chemistry, Cambridge, 2005.
[17] M. Erol, S. Kucukbayrak, A. Ersoy-Mericboyu, M.L. Ovecoglu, Crystallization behaviour of glasses produced from fly ash, Journal of the European Ceramic Society 21 (2001) 2835–2841.
[18] S. Golezardi, V.K. Marghussian, A. Beitollahi, S.M. Mirkazemi, Crystallization behavior, microstructure and dielectric properties of lead titanate glass ceramics in the presence of Bi_2O_3 as a nucleating agent, Journal of the European Ceramic Society 30 (2010) 1453–1460.
[19] R. Magnani, A.T. Adorno, The stability of the Johnson–Mehl–Avrami equation parameters, Journal of Materials Science 30 (1995) 4101–4102.
[20] A. Arora, A. Goel, E.R. Shaaban, K. Singh, O.P. Pandey, J.M.F. Ferreira, Kinetics of ZnO–BaO–B_2O_3–SiO_2 Glass, Journal of Non-Crystalline Solids 354 (2008) 3944–3951.
[21] A.A. Francis, Crystallization kinetics of magnetic glass-ceramics prepared by the processing of waste materials, Materials Research Bulletin 41 (2006) 1146–1154.
[22] A. Karamanov, S. Ergul, M. Akyildiz, M. Pelino, Sinter crystallization of a glass obtained from basaltic tuffs, Journal of Non-Crystalline Solids 354 (2008) 290–295.
[23] D.C. Clupper, L.L. Hench, Crystallization kinetics of tape cast bioactive glass 45s5, Journal of Non-Crystalline Solids 318 (2003) 43–48.
[24] A. Karamanov, M. Pelino, Crystallization phenomena in iron-rich glass, Journal of Non-Crystalline Solids 281 (2001) 139–151.
[25] N.P. Bansal, R.H. Doremus, Determination of reaction kinetic parameters from variable temperature DSC or DTA, Journal of Thermal Analysis and Calorimetry 29 (1984) 115–119.
[26] S. Mahadevan, A. Giridhar, A.K. Singh, Calorimetric measurements on As–Sb–Se glasses, Journal of Non-Crystalline Solids 88 (1986) 11–34.
[27] C. Pãcurariu, M. Litã, I. Lazãu, D. Tita, G. Kovacs, Kineticstudy of the crystallization processes of some glass ceramics based on basalt via thermal analysis, Journal of Thermal Analysis and Calorimetry 72 (2003) 811–821.